European Polymer Journal 186 (2023) 111875

Contents lists available at ScienceDirect

European Polymer Journal

journal homepage: www.elsevier.com/locate/europolj

Photocuring of aliphatic-lineal poly(glycerol adipate) with a monomer bearing thiazolium groups as a promising approach for biomedical applications

V. Hevilla [a,b], A. Sonseca [c,*], C. Echeverría [a,b], A. Muñoz-Bonilla [a,b], M. Fernández-García [a,b,*]

[a] Instituto de Ciencia y Tecnología de Polímeros (ICTP-CSIC), C/Juan de la Cierva, 3, 28006 Madrid, Spain
[b] Interdisciplinary Platform for "Sustainable Plastics towards a Circular Economy" (SUSPLAST-CSIC), Spain
[c] Instituto de Tecnología de Materiales, Universitat Politècnica de València, Camino de Vera, s/n, 46022 Valencia, Spain

ARTICLE INFO

Keywords:
Poly(glycerol adipate)
Enzymatic synthesis
Functionalization
Networks
Antimicrobial
Hemotoxicity

ABSTRACT

In this work, we described the combination of photocurable methacrylic monomer and poly(glycerol adipate) (PGA) macromer to form networks that can be further quaternized to provide antimicrobial character. Both monomers were synthesized enzymatically. Networks with different content of methacrylic monomer were prepared and further characterized by water contact angle measurements, surface charge, soluble fractions, differential scanning calorimetry and microhardness to determine the effect of the methacrylic monomer in the PGA network. Methacrylic monomer affected the mechanical behavior but did not alter the surface wettability, whereas the quaternization did not alter the wettability nor the mechanical properties of the network surfaces. Finally, the obtained network with the introduced permanent cationic charges were tested against Gram-positive *S. aureus* and Gram-negative E. *coli* bacteria showing remarkable antimicrobial activity which increased with the content of methacrylic monomer in the network. Moreover, the assays against red blood cells demonstrated that networks are no toxic.

1. Introduction

Lately, humans are more involved solving the problems of pollution, climate change, environmental degradation, or resource depletion. With this aim, humans turn into biomimicry, which is a practice that learns from and mimics the strategies used by nature. Since the discovery of enzymatic polymerization, enzymes are utilized for the synthesis of linear polyesters/macromers from polyols [1], and diacids or their esters, avoiding gelation due to esterification at secondary hydroxyl groups [2,3]. Polyester polymers made from renewable resources can be used to reduce the high demand for petrochemical products contributing to a large number of applications such as elastomers, sealants, and adhesives, etc. This kind of synthesis also allows the creation of thermoset polyesters, which is a good strategy to obtain amorphous soft materials with low glass transition temperatures. Thermosettings from renewable resources [4,5], normally offer enhanced performance with improved thermal stability, chemical resistance, and structural integrity, enabling fabrication of complex 3D morphologies.

Additive manufacturing or 3D printing has also drawn high research attention in recent years [6], and nowadays 4D printing, process that combines 3D printing with smart materials (self-assembly, multifunctionality, and self-healing) [7,8] has aroused more interest. In the case of stereolithography, which is the first commercialized technology, uses UV lasers as a light source to selectively cure a polymer resin [9,10]. Typically, this process uses oil-based macromers, which cannot be recycled to the crosslinked set. Therefore, it is required the preparation of biodegradable polymeric systems to be attractive for biomedical applications [7,11–13], due to their mechanical properties similar to soft tissues [14,15]. In spite of this, environmentally friendly polymers, biobased and natural, [9] are even more promising materials not only for biomedical applications but also for other technologies such as coatings, adhesive, electronic, energy or manufacturing, among others [16].

Our group has developed several cationic polymethacrylic and polyitaconic systems that contain thiazole groups as a side chain, using conventional and controlled radical polymerization techniques [17–22]. In these polymers the quaternization process originates thiazolium moieties, which is derived from the vitamin (B1) thiamine, as permanent

* Corresponding authors.
E-mail addresses: agsonol@upvnet.upv.es (A. Sonseca), martafg@ictp.csic.es (M. Fernández-García).

https://doi.org/10.1016/j.eurpolymj.2023.111875
Received 19 November 2022; Received in revised form 25 January 2023; Accepted 29 January 2023
Available online 2 February 2023

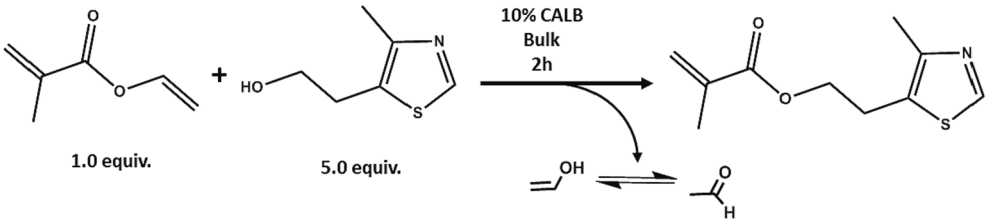

Scheme 1. Enzymatic synthesis of MTA monomer.

cationic charges. This characteristic gives as a result antimicrobial systems [23,24]. Moreover, we have recently described the enzymatic synthesis in a single-step of poly(glycerol adipate) based macromers with varied terminal structure, *viz.* functionality, from reaction of glycerol and divinyl adipate at different stoichiometry ratios [25].

In this paper, we describe the enzymatic synthesis of a photocurable methacrylic monomer and a photocurable telechelic macromer based on the chemical modification of poly(glycerol adipate). The combination of both comonomers gave rise to different networks, which were modified to introduce permanent cationic charges. The structural and thermal characterizations of these networks were performed by water contact angle measurements, and differential scanning calorimetry. Besides, their microhardness analysis was also made to determine the resistance to deformation. Finally, the effectiveness against *Staphylococcus aureus* and *Escherichia coli* bacteria, an ubiquitous pathogenic agent and type of bacteria that lives in our intestines, respectively, was also analyzed by dynamic contact killing.

2. Experimental section

2.1. Materials

Divinyl adipate (DVA, 96,0 %, TCI Europe), glycerol (GLY 99 %, Sigma-Aldrich); vinyl methacrylate (VMA, TCI Chemicals, 98,0%), 5-(2-hydroxyethyl)-4-methylthiazole (Tz, 98 %, Aldrich), iodomethane (MeI, 99.5 %, Merck), acetone (99.5 %, Scharlau), diethyl ether (99.8 %, Honeywell), ethyl acetate (99.8 %, Scharlau), *n*-hexane (96 % Scharlau), 2-benzyl-2-dimethylamino-1-(4-morpholinophenyl)-butanone-1 (Irgacure 369, Ciba Specialty Chemicals), deuterated acetone (99.8 %, Eurisotop), deuterated chloroform (Sigma-Aldrich), N,N-dimethyl formamide (DMF, Scharlau), lithium bromide (LiBr, Sigma Aldrich, >99.9 %), sodium chloride solution (0.9 %, NaCl suitable for cell culture, BioXtra, Sigma Aldrich), phosphate buffered saline powder (PBS, pH 7.4, Sigma Aldrich), fluorescein sodium salt powder (Sigma), and cetyltrimethylammonium chloride (Sigma Aldrich) were used as received. Lipase B from *Candida antarctica* immobilized on microporous

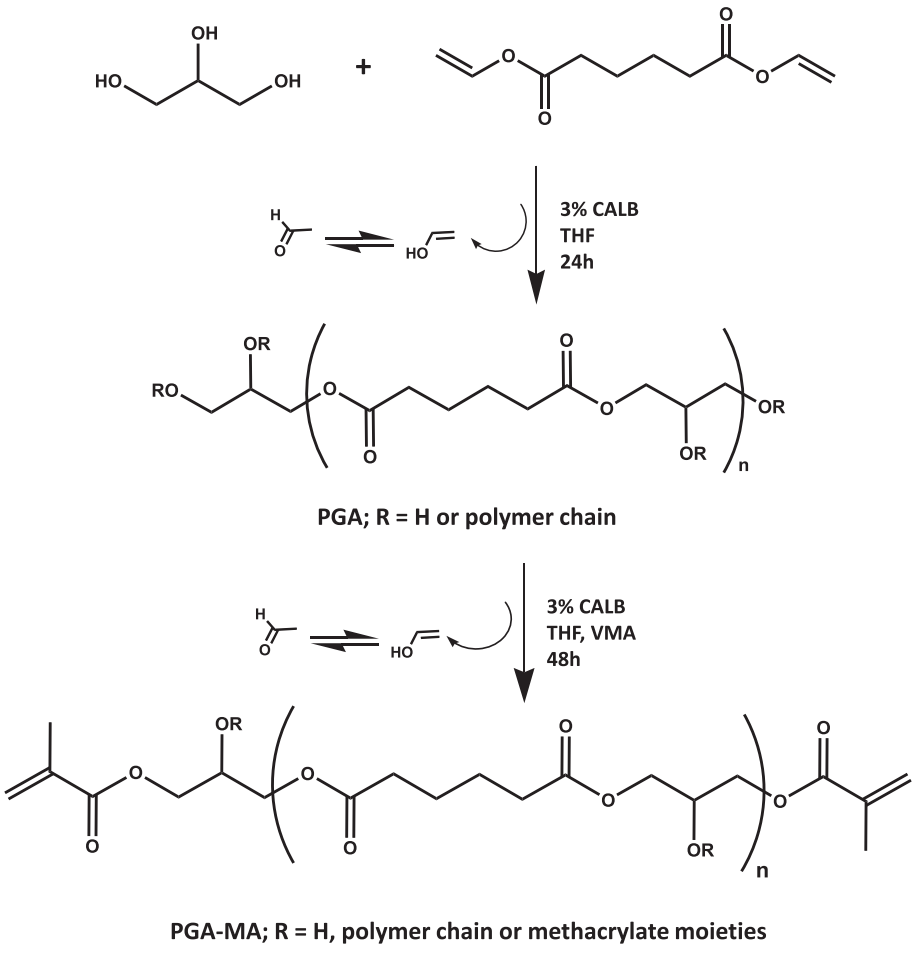

Scheme 2. Synthesis of the PGA and its functionalization to synthesize PGA-MA.

(CALB 5000 U/g, Sigma-Aldrich) was dried during 24 h before its use. For the antibacterial assay, 96 well microplates were purchased from BD Biosciences, Columbia agar (5 % sheep blood) plates were obtained from Fisher Scientific. American Type Culture Collection (ATCC): *Escherichia coli* (*E. coli*, ATCC 25922), and *Staphylococcus aureus* (*S. aureus*, ATCC 29213) were used as bacterial strains and purchased from Oxoid.

2.2. Enzymatic synthesis of 2-(4-methylthiazol-5-yl)ethyl methacrylate (MTA)

MTA was enzymatically synthesized using Tz (0.5629 g, 3.931 mmol) and VMA (2.2039 g, 19.6559 mmol), in presence of 10 wt.% of CALB. The reaction mixture was maintained at 40 °C under argon atmosphere while stirring at 200 rpm. Scheme 1 shows the corresponding reaction of MTA synthesis. After 2 h, the reaction was finished with the addition of cold THF, in order to dilute the reaction mixture and help the removal of lipase CALB by filtration. After that, products were dried using a rotary evaporator and purified by flash column chromatography (hexane to hexane:EtOAc 2:1). MTA was isolated as yellow oil (0.7149 g, 86 % yield). TLC: Rf = 0.41 (hexane/EtOAc, 2:1), ^{1}H NMR (400 MHz, $CDCl_3$, ppm): δ = 8.52 (s, 1H; =CH thiazole), 6.02 (m, 1H; =CH), 5.49 (m, 1H; =CH), 4.22 (t, J = 6.5 Hz, 2H; OCH_2), 3.06 (t, J = 6.5 Hz, 2H; CH_2), 2.33 (s, 3H; CH_3 thiazole), 1.84 (dd, J = 1.2, 1.5 Hz, 3H; CH_3); ^{13}C NMR (400 MHz, $CDCl_3$, ppm): δ = 166.9 (C=O), 149.9 and 149.7 (NCs), 135.9 (—**C**=CH_2), 126.8, 125.8 (=**C**H_2s and C=**C**—S), 64.1, 25.7, 18.3, 14.7.

2.3. Synthesis of poly(glycerol adipate) and its posterior functionalization

The synthesis of poly(glycerol adipate), PGA, was performed following a protocol adapted from Sonseca et al. [25]. Scheme 2 shows the corresponding reactions of synthesis and modification.

PGA synthesis was carried out with a short excess of GLY (GLY/DVA of 1.2/1.0) dissolved in anhydrous THF with a concentration of 730 mg/mL (relative to monomers weight) into a 250 mL flask previously dried. Then, an amount of 3 wt.% of CALB (% relative to monomers weight) was added to the reaction mixture, and this reaction medium was maintained at 40 °C under argon atmosphere while stirring at 200 rpm during 24 h. After that, THF was added to the reaction mixture to finish the reactions and facilitate the filtration of the lipase. The product was dried and dissolved in acetone to precipitate it into an excess of cold diethyl ether. The obtained PGA was recovered by filtration and dried under vacuum until constant weight (81 % of yield), where no residual solvents were detected during characterization. The functionalization of the obtained PGA was carried out by adding the resulting PGA with an excess of VMA of 1/5 (OH/VMA) into a 250 mL flask and stirring at 100 rpm for 1 h to dissolve the reagents dissolved in anhydrous THF (730 mg/mL). When reaction medium was perfectly dissolved, an amount of 3 wt.% of CALB (% relative to reagents weight) was added and the reaction was maintained at 40 °C under argon atmosphere while stirring at 200 rpm during 48 h. After that, THF was added to the flask to dilute the reaction mixture and to remove the enzyme. Then, product (PGA-MA) was precipitated into an excess of cold diethyl ether, filtered and finally dried under vacuum until constant weight (81 % of yield).

2.4. Photo-crosslinking process

PGA-MA macromer was dissolved in acetone forming a solution (initial mixture) with a ratio of 25:75 macromer:solvent in wt.%, with a presence of a photoinitiator (Irgacure® 369, 3.0 wt.% with respect to the total mass of PGA-MA). Besides PGA-MA alone, three different concentrations of MTA (5, 10 and 15 wt.% with respect to PGA-MA mass, i.e., MTA percent would be the 5, 10 or 15 % of the 25 % of the initial mixture, were used to prepare the photocrosslinkable systems (named as nPGA-MA and nPGA-MAx, being x the MTA wt.% with respect to PGA mass). Obtained mixtures were protected from light and stirred for 5 min at room temperature. Then, 50 μL of initial mixture were added on circular glass plates (used as support) with a diameter of 12 mm. This volume was chosen because it was the volume that allowed obtaining a homogeneous coating of the plate. Later, they were dried for 20 min in a fume hood, allowing the solvent to evaporate. Subsequently, they were exposed to an UV lamp using a UVPTM CL–1000 short-wave photocrosslinker (λ = 313 nm) for 10 min, producing the crosslinked samples. The UV-cured films have a thickness of 54 ± 5 μm and weight of 4.3 ± 0.5 mg.

2.5. Quaternization of crosslinked samples

Photocrosslinked samples (nPGA-MAx) were washed repeatedly with MeOH, and quaternized with 10 μL of MeI in 1.0 mL of MeOH under absence of light at 40 °C. After 3 weeks, samples were extracted of the medium and subjected to a new sequence of washes with MeOH, and dried under vacuum until constant weight (named as nPGA-MAxQ).

2.6. Characterization

2.6.1. Nuclear Magnetic Resonance (NMR)

^{1}H spectra were recorded on a Bruker Avance III HD-400AVIII spectrometer at room temperature using acetone-d_6 and tetramethylsilane (TMS) as internal reference for reported chemical shifts.

2.6.2. Size exclusion chromatography (SEC)

Relative molecular weights of PGA and PGA-MA were determined by *SEC* using a Waters Division Millipore system equipped with a Waters 2414 refractive-index detector, using N,N-dimethylformamide (Scharlau, 99.9 %) containing 0.1 % of LiBr as the eluent at a flow rate of 1 mL/min at 50 °C. Poly(methyl methacrylate) standards (Polymer Laboratories Ltd., Church Stretton, UK) were used to calibrate the system ranging from 1.4 10^6 and 5.5 10^2 g/mol.

2.6.3. Fourier transform infrared (FTIR)

FTIR spectra were recorded between 400 and 4000 cm^{-1} spectral range with a 4 cm^{-1} resolution with a Perkin Elmer Spectrum Two instrument equipped with an attenuated total reflection module (ATR). A background spectrum was acquired before every sample and all samples were vacuum-dried prior to measurement.

2.6.4. Contact angle

Static water contact angle (WCA) of the samples was determined on the surface of the prepared films using a KSV Theta goniometer (KSV Instruments Ltd.) in contact mode at 25 °C. The contact angle was measured at least eight times on different sites of the surface using a volume of the drops of 3.0 μL. Each data reported is the average of eight measurements ± SD (standard deviation).

2.6.5. Differential scanning calorimetry (DSC)

Thermal data were obtained by DSC with a TA Instruments Q2000 series equipped with a refrigerated cooling system (RCS). Experiments were conducted under a flow of dry nitrogen with a sample weight of approximately ~ 2 mg. The samples were equilibrated at −60 °C and heated to 200 °C at 10 °C/min, then, rapidly cooled to −60 °C and again heated to 200 °C.

2.6.6. Microhardness (MH)

Microindentation measurements were performed using a Vickers indenter attached to a Leitz microhardness tester. A contact load of 0.96 N for a time of 25 s was employed. Microhardness (MH) values in MPa were calculated according to the relationship [26]:

$$MH = 2\sin 68^{\circ}\left(\frac{P}{d^2}\right)$$

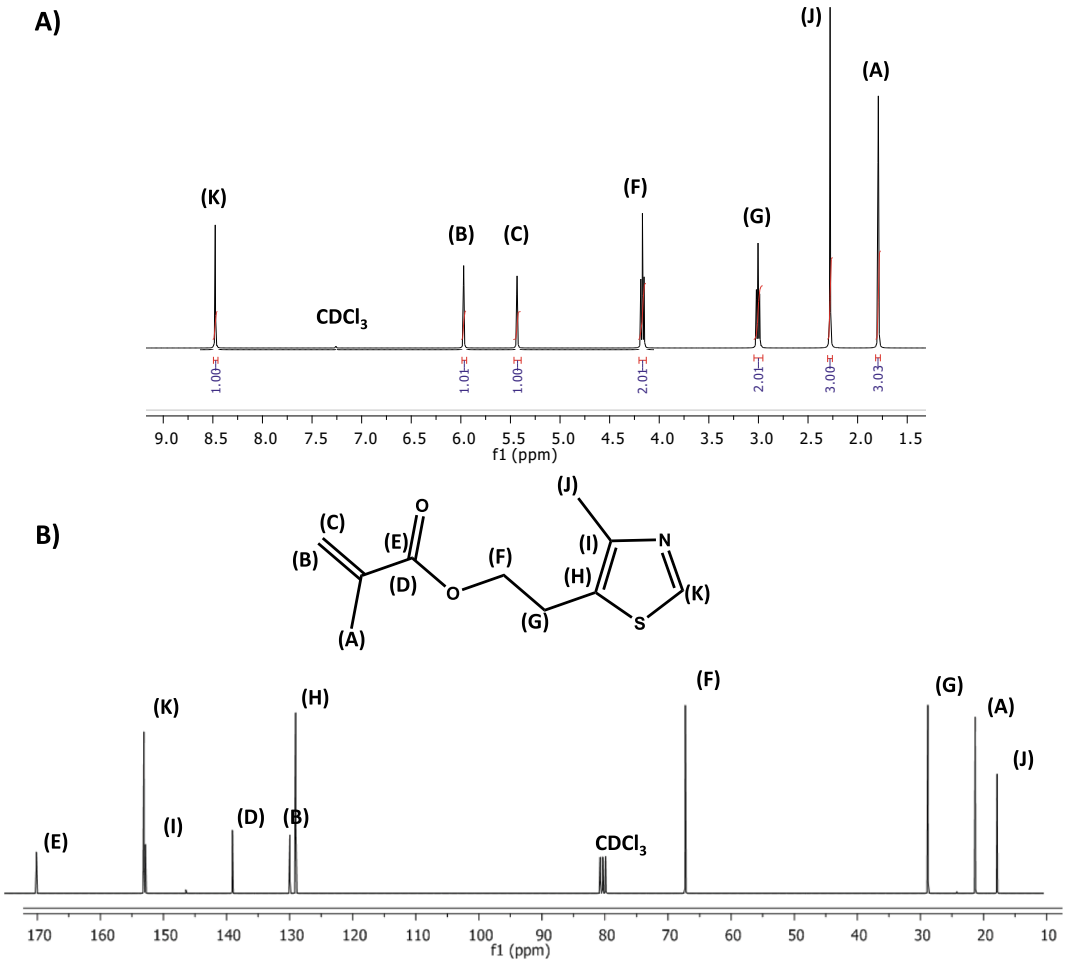

Fig. 1. (A) ^{1}H NMR and (B) ^{13}C NMR spectra of synthesized MTA monomer.

where P is the contact load and d is the diagonal length of the projected indentation area (in N and mm, respectively). Diagonals were measured in the reflected light mode within 30 s of load removal, using a digital eyepiece equipped with a Leitz computer-counter-printer (RZA-DO). Each data reported is the average of several measurements ± SD (standard deviation).

2.6.7. Surface charge

Surface charge was measured following a method previously described in the literature [27,28]. Films were placed in 1.0 mL of 1 wt. % aqueous sodium fluorescein solution for 10 min. After that, samples were washed extensively with distilled water under stirring. Then, the fluorescein was desorbed from the sample by treating the film with 1.0 mL of 0.1 wt.% of CTAC solution for 10 min with shaking at 200 rpm. This was repeated other two times. Subsequently, the amount of fluorescein obtained in the extraction was determined with the value of absorbance at 501 nm measured by UV–vis spectroscopy (Lamda 35, PerkinElmer) in a solution prepared by adding 0.3 mL of 100 mM phosphate buffer (pH 8.0). And the concentration of fluorescein was calculated with an extinction coefficient [29] of 77 M^{-1} cm^{-1} assuming a relationship of 1:1 for fluorescein to each accessible cationic thiazolium group.

Statistical analysis. The analysis of variance (ANOVA) was performed to detect any significant differences between the factors at $p < 0.05$. The software used was Origin 8.5 (Northampton, MA 01060, USA).

2.7. Antibacterial and hemolytic assays

The antibacterial activity of the different UV-cured nPGA-MAxQ films was measured following the E2149-20 standard method from the American Society for Testing and Material (ASTM) [30] against *E. coli* and *S. aureus*. The same procedure was carried out with nPGA-MA (films without MTA) and nPGA-MAx networks. As blank control experiment, the test was performed in absence of films. The study consisted of culture both bacterial cells on 5 % sheep blood Columbia agar plates for 24 h at 37 °C. After that, the bacterial suspensions were prepared in saline medium using the McFarland turbidity scale and further diluted to $\times 10^{6}$ colony-forming units (CFU)/mL with PBS. Next, 1.0 mL of the tested inoculum and 9.0 mL of PBS to reach a working solution of $\sim 10^{5}$ CFU/mL were placed in sterile falcon tubes, which contained the UV-cured films. nPGA-MA films and nPGA-MA5, nPGA-MA10 and nPGA-MA15 were used as blank control experiments, and also in the absence of films, remaining submerged in the solution. Suspensions were shaken at 120 rpm for 24 h. After that, 100 µL from each bacterial suspension were placed in the first column of a 96-well round-bottom microplate and 90 µL of PBS was added into the rest of the wells. From the first column, 10 µL of bacterial suspension were taken and added to the second column, and it was diluted by 10-fold serial dilutions in the rest of the wells. Finally, the colonies were counted by the plate counting method, and the reduction percentage was calculated in comparison to the control, following the Equation 1. All the measurements were made in triplicate.

$$\textit{Percentage of bacteria kill} = (A - B)/A \times 100\% \quad (1)$$

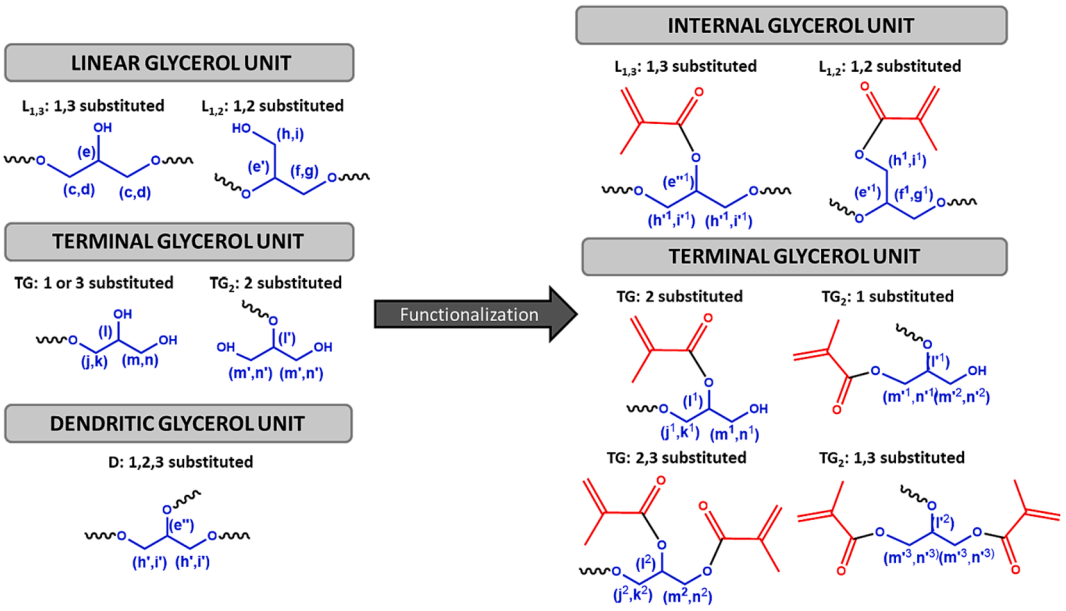

Fig. 2. ^{1}H NMR proton assignments for linear, terminal and dendritic glycerol units contained in the polymers, free or with methacrylate moieties.

where *A* is CFUs of blank control and *B* is CFUs after the contact with the UV-cured films.

Human Red Blood Cells (RBC), were collected in heparinized-tubes from healthy donors and were centrifuged at 3100 rpm for 10 min and washed three times with cold PBS to remove plasma and white blood cells. The solution was suspended to 5 % (v/v) in the PBS to yield the RBC stock suspension and used immediately. Each network (4.3 ± 0.5 mg) was added to a tube with 4 mL of RBC solution. Positive control (100 % hemolysis) was checked by adding 1 mL of Triton X-100 solution and negative control (0 % hemolysis) was performed by adding 3 mL of RBC stock in 1 mL of PBS. The tubes were incubated at 37 °C for 1 h and 24 h and centrifuged then at 3100 rpm for 10 min to settle the non-lysed cells. Then, 150 μL of supernatant from each tube was added into a sterile 96-well microplate and the absorbance of wells was measured at 550 nm. Percentage of hemolysis was determined as.

follows:

$$Hemolysis(\%) = (A - A_0)/(A_{100} - A_0) \times 100 \quad (2)$$

where A is the absorbance of the analyzed network, A_0 the absorbance of the negative control (0 % hemolysis) and A_{100} the absorbance of the positive control (100 % hemolysis). Each percentage is given as the average and standard errors from different experiments performed in triplicates.

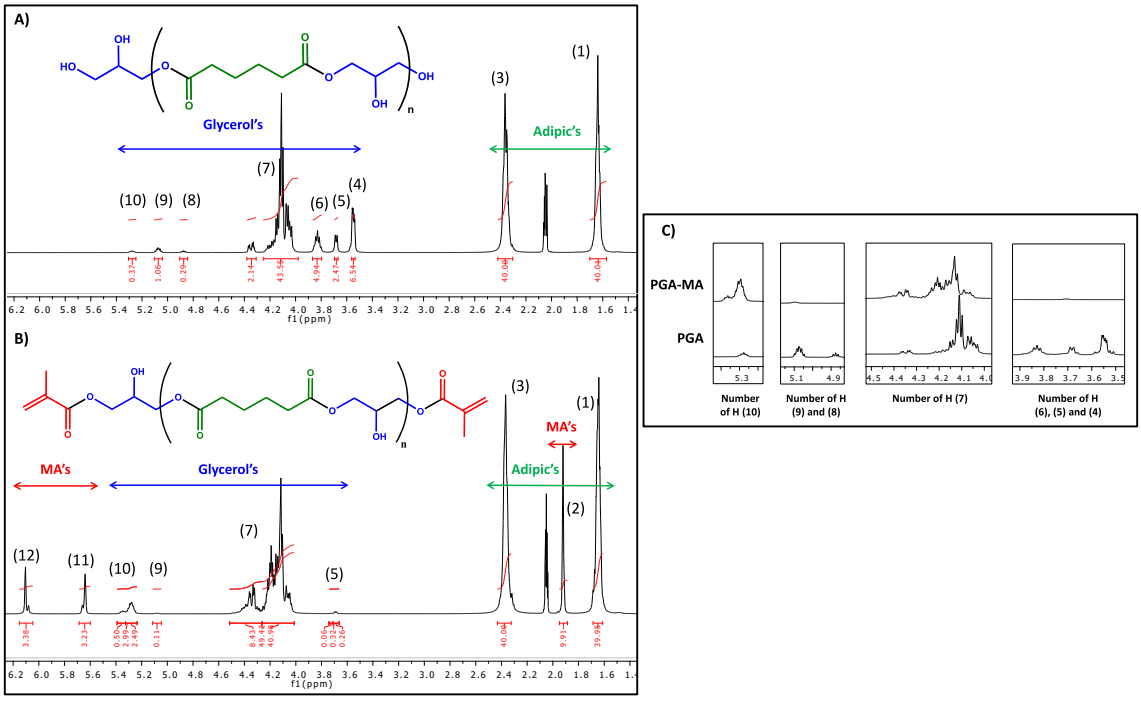

Fig. 3. ^{1}H NMR spectra of (A) PGA, (B) PGA-MA and (C) expansions of ^{1}H NMR spectra of synthesized PGA and PGA-MA where different units of glycerol are distinguished.

Table 1
^{1}H NMR Signal integrals and shifts of the different protons of both polymers: PGA and PGA-MA.

Number of signal	Proton PGA	Number of H	δ (ppm)	Integral [I]	Proton PGA-MA	Number of H	δ (ppm)	Integral [I]
1	b	4	1.6	40.0_0	b	4	1.6	40.0_0
2	s	3	–	–	s	3	1.9	9.9_1
3	a	4	2.4	40.0_0	a	4	2.4	40.0_0
4	m, n	2	3.5	6.5_4	m, n; m^1n^1; m^2n^2	2	–	0.0_0
5	h, i	2	3.7	1.3_1	h, i; h^1i^1	2; 2	3.7	0.2_6
	m', n'	4		1.1_6	m',n'	4		0.0_0
					m'^1,n'^1; m'^2,n'^2; m'^3,n'^3	4; 4; 4		0.0_6
6	l	1	3.8	4.9_4	l	1	–	0.0_0
7	j, k	2	4.4–4.0	6.5_4	j, k; j^1k^1; j^2k^2	2; 2; 2	4.5–4.0	48.2_3
	c, d, e	5		35.5_3	c, d, e,	5		
	h', i'	4		1.4_8	h', i'; $h'^1i'^1$	4; 4		
	f,g	2		1.9_8	f,g; f^1g^1	2		0.0_2
8	l'	1	4.9	0.2_9	l'	1	–	0.0_0
9	e'	1	5.1	1.0_6	e'; e'^1; e'^2	1	5.08	0.1_1
10	e'	1	5.3	0.3_7	e'; e'^1; e'^2; l^2	1	5.32	2.9_9
11	r'	1	–	0.0_0	r'	1	5.64	3.2_3
12	r	1	–	0.0_0	r	1	6.10	3.3_8

3. Results and discussion

3.1. Synthesis and characterization of enzymatically synthesized compounds

First, MTA monomer has already been synthesized by Tejero et al. [22] via reaction between 5-(2-hydroxyethyl)-4-methylthiazole and 2-methylpropenoic acid using anhydrous acetonitrile, N,N′-dicyclohexylcarbodiimide and 4-dimethylaminopyridine. However, we have managed to synthesize the monomer by means of a transesterification catalyzed by CALB with the same derivative of thiazole but with vinyl methacrylate. Thus, the reaction is carried out with only 2 h and in the absence of solvent. It is also worth mentioning that the separation of CALB by filtration allows obtaining the reaction medium without residues or catalysts. In turn, it facilitates the purification of the different obtained products. These are the MTA monomer and the residual VMA that has not reacted. The separation of both components was made by flash column chromatography. Fig. 1 shows ^{1}H and ^{13}C NMR of the MTA monomer with assigned and integrated peaks.

Secondly, the synthesis of PGA from DVA and GLY in THF with CALB was successfully performed. The M_n and Đ obtained by *SEC* were 4600 g/mol and 1.4, respectively. These parameters are within the values that are reported in the literature under the same reaction conditions [31]. Chemical compositions of the PGA and PGA-MA were determined by ^{1}H NMR; technique which also has been used to analyze the end-groups of low molecular weight polymers [25]. Fig. 2 illustrates the assignments for terminal glycerol protons (TG and TG_2) and glycerol units contained in linear ($L_{1,3}$ and $L_{1,2}$) and dendritic polymer chains, and also the assignments for the different glycerol protons functionalized with methacrylate moieties.

Fig. 3 shows the ^{1}H NMR spectra of synthesized polymers: PGA (A) and PGA-MA (B). PGA spectrum shows CH_2 adipic protons (**a, b**) that appear in the spectral range between 1.6 and 2.5 ppm, but the spectrum does not show vinyl proton, which would be seen at ~ 7.30, 4.90 and 4.60 ppm. This confirms that the majority of polymer end-groups are hydroxyl groups, corresponding to glycerol. All protons related to glyceride repeating units are found between 3.5 and 4.5 ppm, where the multiplets in the region of 3.5–3.9 ppm correspond to glycerol units: (**l**), (**h, i**), (**m, n**), and (**m', n'**), while peaks at 5.1 and 5.3 ppm are related to 1,2-substituted (**e′**), and 1,2,3-substituted glycerides (dendritic, **e″**), respectively, being the latest produced due to the lack of regioselectivity of the enzyme during the reaction. The amount of dendritic units in the polymer can be calculated from ^{1}H NMR as the amount of 1,2,3-substitued glycerol following the Eq (2):

$$1,2,3-substituted\ units(\%) = \frac{I_{e''}/n_{e''}}{I_a/n_a}\cdot 100 \quad (2)$$

where I is the intensity and n is the number of protons.

The obtained value is 3.9 %, which means that more than 96 % of repeating units are disubstituted; therefore, the polymer chain can be considered as lineal.

Spectrum of PGA-MA shows new peaks at 6.1, 5.7 and 1.9 ppm that correspond to MA moieties. The functionalization degree, i.e. the methacrylation degree, was obtained by comparing the signal integrals of the adipic methylene groups (1.7 ppm) with the signal intensity of the

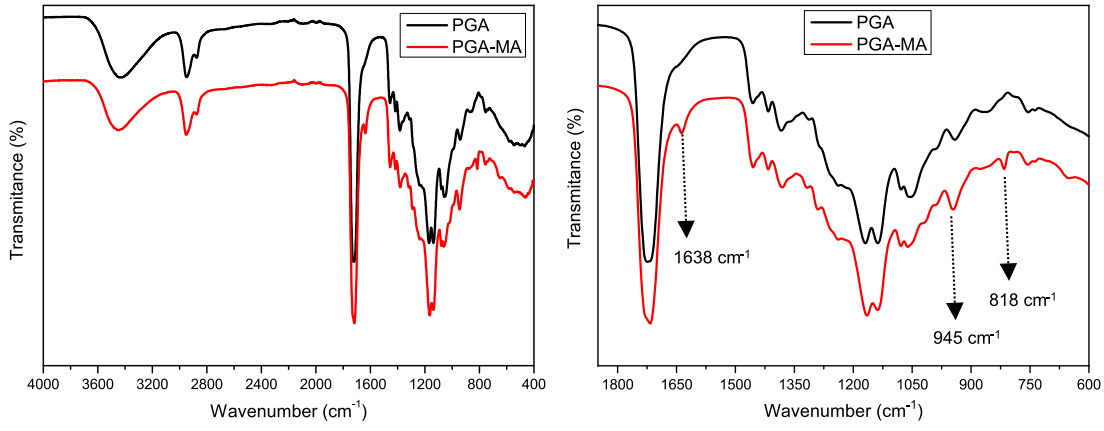

Fig. 4. Right: complete ATR–FTIR spectra of the PGA and PGA-MA. Left: magnified view of the 1800–600 cm^{-1} region.

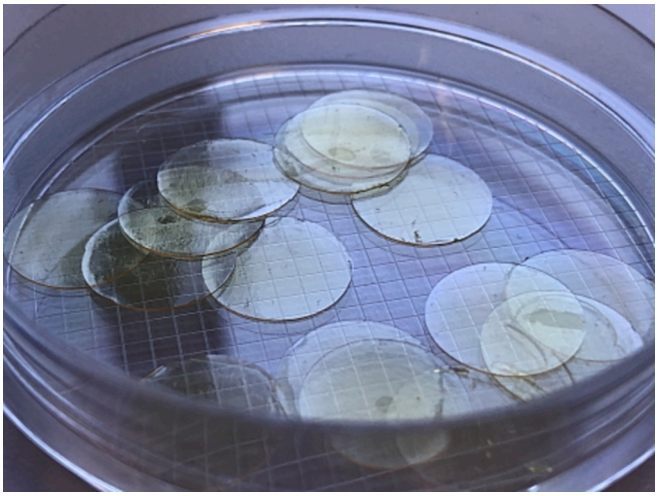

Fig. 5. Cured samples of PGA-MA with MTA, nPGA-MAx networks.

Table 2
Surface properties, i.e. sol fraction, surface charge, water contact angle (WCA) and microhardness (MH) of nPGA-MA films with different MTA content without and with quaternization. The superscript letters represent significant differences with a $p < 0.05$.

Sample	Sol (wt.%)	Charge (N^+/cm^2)	WCA (°)	MH (MPa)
nPGA-MA	8.2 ± 0.28[a]	–	69.70 ± 2.56[a,c]	1.17 ± 0.10[a]
nPGA-MA5	7.8 ± 0.21[a]	–	74.02 ± 3.90[b,c]	1.82 ± 0.42[b]
nPGA-MA5Q	–	(1.07 ± 0.18)·10^{17} [a]	73.39 ± 2.62[b,c]	0.82 ± 0.09[a]
nPGA-MA10	5.7 ± 0.19[b]	–	74.48 ± 2.75[b]	2.38 ± 0.44[c]
nPGA-MA10Q	–	(3.98 ± 0.25)·10^{17b}	74.50 ± 3.96[b]	1.03 ± 0.09[a]
nPGA-MA15	3.3 ± 0.10[c]	–	67.76 ± 2.73[a]	2.71 ± 0.30[d]
nPGA-MA15Q	–	(9.57 ± 1.17)·10^{17c}	71.41 ± 2.91[c]	1.55 ± 0.22[b,e]

methacrylate groups. The resulting value was found to be 33 ± 1 % of the methacrylation degree. Thus, this functionalization provokes the disappearance of the signal at 4.9 ppm (**l'**) and the disappearance of the majority of proton signals in the region of 3.5–3.9 ppm: (**l**), (**h, i**), (**m', n'**) and (**m, n**) (see Fig. 3C). Therefore, the functionalization has occurred predominantly in the primary hydroxyl groups of terminal and 1,2 linear substituted glycerol units. Besides, new signals appear at around 5.4 ppm and 4.2 ppm that is indicative of the appearance of new kind of protons (r, r' of the double bond and s of CH_3 of methyl) related to the functionalization of glycerol units with methacrylate moieties. Table 1 collects the integral of the different the proton signals for PGA and PGA-MA polymers.

Fig. 4 shows the ATR–FTIR spectra of the PGA and PGA-MA. Regarding the spectra, both compounds have several peaks in common. Among these peaks, they were showing a broad peak at 3450 cm^{-1} associated with the stretching vibration of hydroxyl groups, a few bands at 2950 cm^{-1} and 2870 cm^{-1} corresponding to symmetric and asymmetric stretching of alkyl C—H bonds of methyl and alkane groups. Below 2000 cm^{-1}, they showed a band at 1725 cm^{-1} associated with the stretching of carbonyl group and around 1170–1120 cm^{-1} the stretching peak of carboxyl group appears. The modification reaction generates new ones, associated with the methacrylate groups, such as the peaks at 818 cm^{-1} (C═CH_2 twisting), 945 cm^{-1} (═C—H bending), and 1638 cm^{-1} (C═CH_2 stretching) [32,33].

3.2. Preparation and characterization of photocured networks based on PGA-MA.

The synthesized PGA-MA polymer was dissolved under the presence of three different amounts of MTA and Irgacure® 369 initiator in acetone. Then, the mixture was added to glass disks and cured with UV light radiation during 10 min. After that, the samples were immersed in methanol to be easily removed from the glass (see Fig. 5). Methanol was also used in the quaternization process. To confirm that there is no leaking of polymer during the quaternization process, the networks were exposed to an extraction process by immersion of the films in methanol during one week. Table 2 shows, among others properties, the sol fraction of UV-cured films, which reduced from 8.2 % to 3.2 % accordingly with the increase of MTA contents. It indicated that incorporation of MTA improved the crosslinking density of PGA-MA.

The synthesized PGA is considered as linear, with around 33 % of hydroxyl groups are substituted by methacrylate moieties (substitution mainly at primary hydroxyl groups of terminal units and 1,2 linear substituted glycerol units). Therefore, the addition of a small molecule with another crosslinkable bond would produce an increase in the degree of crosslinking, generating a 3D network with higher density.

3.2.1. Chemical analysis of the photocured networks based on PGA-MA

FTIR spectra were performed to confirm the crosslinking process. Fig. 6 shows the spectra of different networks and the uncured PGA-MA. The disappearance of the peak at 1637 cm^{-1}, characteristic of methacrylate moieties, confirms the crosslinking of the systems.

Knowing that the sol% of the samples was low, the quaternization of the films was carried out with an *N*-alkylation reaction with

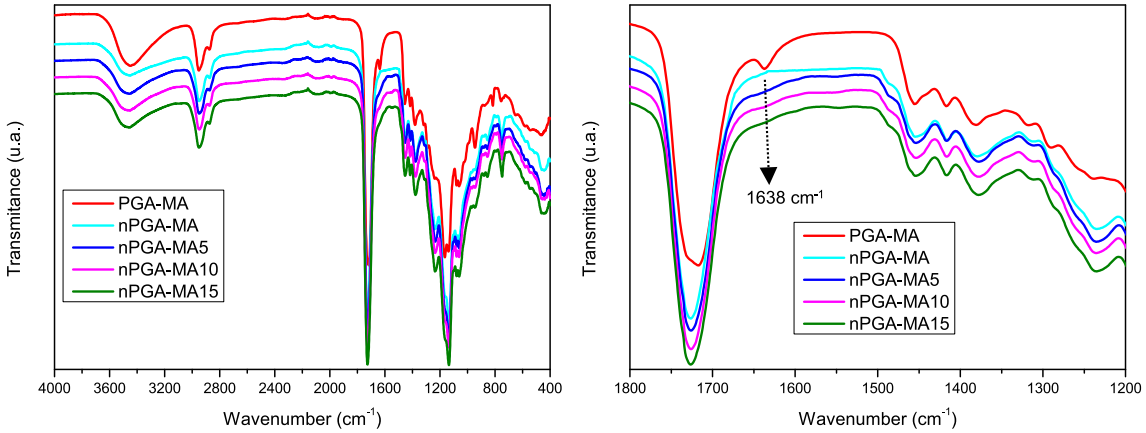

Fig. 6. Right side: complete ATR–FTIR spectra of nPGA-MAx networks and the nPGA-MA. Left side: magnified view of the 1800–600 cm^{-1} area.

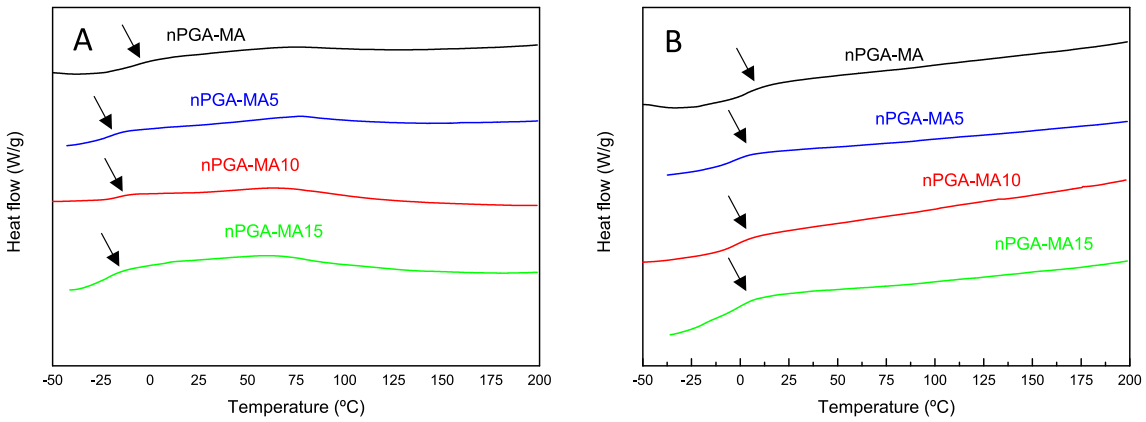

Fig. 7. DSC thermograms of nPGA-MA based networks, where the $T_{g,i}$ and $T_{g,\infty}$ are marked with arrows. (A) First heating run and (B) second heating run of nPGA-MAx networks.

iodomethane to produce the corresponding thiazolium groups. Nitrogen quaternization of thiazole groups is formed to provide antimicrobial character to these materials [34,35]. It is important to mention that previous quaternization of monomer was performed but this fact incapacitates its crosslinking with the polymer.

To confirm that the quaternization of the films with MTA was successful, the accessible cationic units on the surface were measured using a method based on the adsorption of fluorescein by cationic units. Later, adsorbed fluorescein was desorbed with CTAC and quantified by UV–vis spectroscopy. Obtained values of cationic groups by this technique are shown in Table 2, whose are higher that previously determined for other contact-active surfaces and high above from the threshold required to be active [28,27]. As expected, the surface charge values are higher as the percentage of MTA increases in the network.

3.2.2. Contact angle measurements

It is well known that the hydrophilic/hydrophobic balance of the material is one of the key roles in biomaterial behavior when it is placed in the body. Therefore, the films were evaluated by water contact angle measurements (see Table 2). It is easily observed that all values are lower than 90°, so the surfaces can be considered as hydrophilic surfaces. Having in mind that the synthetized PGA-MA is rather linear, hydroxyl free groups are more available due to spatial rearrangement; hence, enhance the hydrophilicity. Comparatively, crosslinked nPGA-MA polymer presents similar value 69.70 ± 2.56° that those reported in the literature for PGA depending on the branching degree [36]. The addition of MTA comonomer in the network slightly increases the hydrophobicity but when the MTA amount is 15 wt.% the hydrophilic part seems to influence and presents similar value to network without MTA units. The quaternization process provokes some adjustments but the differences between them are very small.

3.2.3. Microhardness measurements

The mechanical properties of the crosslinked polymers were studied by microhardness test to study the effect of the incorporation of MTA and its quaternization on the elastic recovery or the resistance to plastic deformation of these materials. The MH results are also shown in Table 2 and as can be observed, the incorporation of the different amounts of MTA into the system causes the increment of MH values with respect to the nPGA-MA value, being this increment higher as the amount of MTA augment. This fact could be due to existence of more crosslinking points in the network, increasing the stiffness of the films. Conversely, when these films are quaternized the MH average markedly decreased, although the tendency is the same. This fact could be explained by the cleavage of inter- and intramolecular interactions of the networks due to the formation of quaternary nitrogen in the film with the incorporation of a methyl group on the system, which make the network less rigid.

Table 3
Thermal properties of nPGA-MA films with different MTA content without and with quaternization. The errors of the temperature are equal to ±0.5 °C.

Sample	$T_{g,i}$ (°C)	$T_{g,\infty}$ (°C)
nPGA-MA	−8.5	5.0
nPGA-MA5	−20.5	−1.0
nPGA-MA5Q	−19.5	−1.5
nPGA-MA10	−17.5	−2.5
nPGA-MA10Q	−17.5	−2.0
nPGA-MA15	−21.5	−4.5
nPGA-MA15Q	−20.0	−4.5

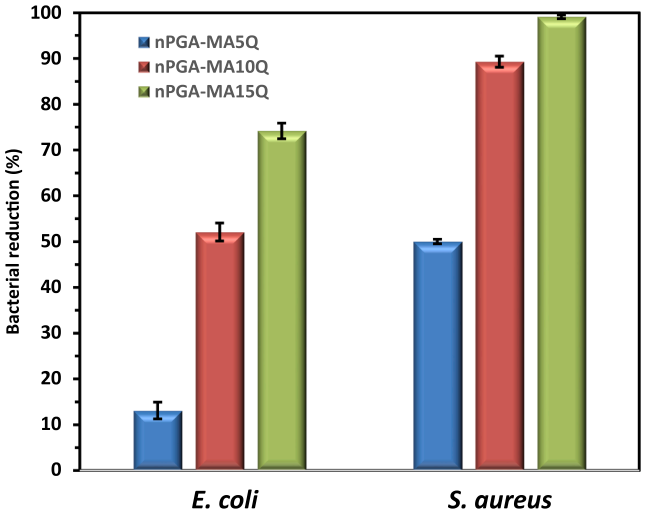

Fig. 8. Antibacterial activity expressed as the percentage of bacterial reduction of PGA-MA based networks against *S. aureus* and *E. coli* bacteria after 24 h of contact time.

3.2.4. Thermal analysis

Followed, the thermal study by thermal scanning calorimetry of non-quaternized nPGA-MAx and quaternized nPGA-MAxQ networks were performed. DSC profiles of first heating and second heating curves corresponding to nPGA-MAx are displayed in Fig. 7. The different transitions are collected in Table 3. The transition showed in the curve at −8.5 °C for nPGA-MA corresponds to the initial glass transition ($T_{g,i}$), which decreases as MTA amount increases in the network. For all the films an exothermic event after glass transition indicates some uncured fraction. In the second heating run, the glass transition temperature ($T_{g,\infty}$) increases to near 0 °C and the residual uncured fraction is

Table 4
Hemotoxicity percentage values of nPGA-MAx and nPGA-MAxQ networks against red blood cells after 1 h and 24 h of contact.

Sample	Hemolysis (%) 1 h	Hemolysis (%) 24 h
nPGA-MA5	1.7 ± 0.9	0.7 ± 0.1
nPGA-MA5Q	0.3 ± 0.1	0.5 ± 0.1
nPGA-MA10	1.7 ± 0.1	3.4 ± 0.1
nPGA-MA10Q	0.3 ± 0.2	0.5 ± 0.2
nPGA-MA15	0.4 ± 0.2	0.5 ± 0.1
nPGA-MA15Q	0.2 ± 0.1	0.3 ± 0.1

suppressed [37]. The DSC profiles of quaternized networks are quite similar to non-quaternized ones, which indicates the modification does not significantly altered the thermal properties of the networks. To confirm that there is no leaking of polymer during the quaternization process, the networks were exposed to an extraction process by immersion of the films in methanol during one week. There were no solid residues after the procedure, which indicated that there were not free polymer chains.

3.3. Antibacterial and hemolytic assays

Additionally, the antimicrobial activity assays the nPGA-MA based networks were carried out. Films were subjected to study against Gram positive *S. aureus* and Gram negative *E. coli* strains. In the antibacterial test, the circular films with an area of 0.85 cm^2 were inoculated in 10 mL of bacterial suspension (~10^5 CFUs). In addition, non quaternized films and the nPGA-MA without MTA were also tested as controls. Fig. 8 displays the percentage reduction against bacteria for all the samples, being 100 % the completely reduction of bacteria and 0 % the null antibacterial activity. It is noticeable that only the quaternized films caused a notable reduction in bacteria, which is more evident as MTA content increases. A higher antimicrobial activity of films with 15 % of MTA was expected due to the higher superficial charge of the network. Moreover, these crosslinked materials are more effective against *S. aureus* than towards *E. coli* bacteria, as it is expected since they present different cell wall nature and is easier to attack a single membrane than a double [38].

The toxicity test was performed to the networks against RBC for 1 h and 24 h and the results are displayed in Table 4. As can be seen, the quaternized and non-quaternized networks are practically no hemolytic, which indicates that there are no toxic.

4. Conclusions

The enzymatic functionalization of PGA with methacrylic moieties allowed its posterior photocuring. The incorporation of enzymatic synthetized MTA monomer into the network clearly influences the mechanical behavior but does not significantly altered the surface wettability. The quaternization reaction practically does not modify the wettability and neither the microhardness of the network surfaces. However, this modification introduces positive charges and a new character to the systems, viz. antimicrobial activity. This activity is stronger against Gram-positive bacteria than Gram-negative and increases as MTA content does. Moreover, these networks are no toxic against red blood cells. Therefore, these networks could be useful for the development of scaffolds in 3D photoprinting technology, such as, prostheses or screw or pins in internal fixation.

CRediT authorship contribution statement

V. Hevilla: Writing – original draft, Investigation, Writing – review & editing. **A. Sonseca:** Conceptualization, Methodology, Funding acquisition. **C. Echeverría:** Investigation, Writing – review & editing, Funding acquisition. **A. Muñoz-Bonilla:** Investigation, Writing – review & editing, Funding acquisition. **M. Fernández-García:** Conceptualization, Methodology, Writing – original draft, Writing – review & editing, Funding acquisition.

Declaration of Competing Interest

The authors declare that they have no known competing financial interests or personal relationships that could have appeared to influence the work reported in this paper.

Data availability

The authors confirm that the data supporting the findings of this study are available within the article.

Acknowledgements

AS acknowledges her "APOSTD/2018/228" and "PAID-10-19" postdoctoral contracts from Culture and Sport Council from the Government of Valencia, and from the Polytechnic University of Valencia, respectively).

Funding

This work was funded by the MICINN (project PID2019-104600RB-I00), the Agencia Estatal de Investigación (AEI, Spain) and Fondo Europeo de Desarrollo Regional (FEDER, EU) and by the Valencian Autonomous Government, Generalitat Valenciana, GVA (GV/2021/182).

References

[1] K. Lang, R.J. Sánchez-Leija, R.A. Gross, R.J. Linhardt, Review on the impact of polyols on the properties of bio-based polyesters, Polymers (Basel) 12 (2020) 1–25.
[2] S.-I. Shoda, H. Uyama, J.-I. Kadokawa, et al., Enzymes as green catalysts for precision macromolecular synthesis, Chem Rev 116 (2016) 2307–2413, https://doi.org/10.1021/acs.chemrev.5b00472.
[3] V. Hevilla, A. Sonseca, C. Echeverría, et al., Enzymatic synthesis of polyesters and their bioapplications: recent advances and perspectives, Macromol. Biosci. 21 (2021) 1–28, https://doi.org/10.1002/mabi.202100156.
[4] J.M. Raquez, M. Deléglise, M.F. Lacrampe, P. Krawczak, Thermosetting (bio) materials derived from renewable resources: a critical review, Prog. Polym. Sci 35 (2010) 487–509, https://doi.org/10.1016/j.progpolymsci.2010.01.001.
[5] B.B. Risley, X. Ding, Y. Chen et al., Citrate crosslinked poly(glycerol sebacate) with tunable elastomeric properties. Macromol. Biosci. 10.1002/MABI.202000301.
[6] X. Kuang, K. Chen, C.K. Dunn, et al., 3D Printing of highly stretchable , shape-memory and self-healing elastomer toward novel 4D printing (2018), 10.1021/acsami.7b18265.
[7] F. Momeni, S.M. Mehdi, N. Hassani, X. Liu, J. Ni, A review of 4D printing, Mater. Des. 122 (2017) 42–79, https://doi.org/10.1016/j.matdes.2017.02.068.
[8] P. Fu, H. Li, J. Gong, et al., 4D printing of polymers: techniques, materials, and prospects, Prog. Polym. Sci. 126 (2022), 101506, https://doi.org/10.1016/j.progpolymsci.2022.101506.
[9] C. Yu, J. Schimelman, P. Wang, et al., Photopolymerizable biomaterials and light-based 3D printing strategies for biomedical applications, Chem. Rev. (2020), https://doi.org/10.1021/acs.chemrev.9b00810.
[10] E. Blasco, M. Wegener, C. Barner-Kowollik, Photochemically driven polymeric network formation: synthesis and applications, Adv. Mater. 29 (2017), https://doi.org/10.1002/adma.201604005.
[11] C. Lin, J. Lv, Y. Li, et al., 4D-printed biodegradable and remotely controllable shape memory occlusion devices, Adv. Funct. Mater. 29 (2019), https://doi.org/10.1002/adfm.201906569.
[12] A.S. Wu, W. Small, T.M. Bryson, et al., 3D printed silicones with shape memory, Sci. Rep. 7 (2017) 1–6, https://doi.org/10.1038/s41598-017-04663-z.
[13] J.L. Ifkovits, J.A. Burdick, Review: photopolymerizable and degradable biomaterials for tissue engineering applications, Tissue Eng. 13 (2007) 2369–2385, https://doi.org/10.1089/ten.2007.0093.
[14] S. Chen, Z. Wu, C. Chu, et al., Biodegradable elastomers and gels for elastic electronics, Adv. Sci. 9 (2022) 1–27, https://doi.org/10.1002/advs.202105146.
[15] S. Pashneh-Tala, R. Owen, H. Bahmaee, et al., Synthesis, characterization and 3D micro-structuring via 2-photon polymerization of poly(glycerol sebacate)-methacrylate-an elastomeric degradable polymer, Front. Phys. 6 (2018), https://doi.org/10.3389/fphy.2018.00041.
[16] R. Ding, Y. Du, R.B. Goncalves, et al., Sustainable near UV-curable acrylates based on natural phenolics for stereolithography 3D printing, Polym. Chem. 10 (2019) 1067–1077, https://doi.org/10.1039/c8py01652f.
[17] A. Chiloeches, C. Echeverría, R. Cuervo-Rodríguez, et al., Adhesive antibacterial coatings based on copolymers bearing thiazolium cationic groups and catechol moieties as robust anchors, Prog. Org. Coat. 136 (2019), 105272, https://doi.org/10.1016/j.porgcoat.2019.105272.

[18] R. Cuervo-Rodríguez, A. Muñoz-Bonilla, F. López-Fabal, M. Fernández-García, Hemolytic and antimicrobial activities of a series of cationic amphiphilic copolymers comprised of same centered comonomers with thiazole moieties and polyethylene glycol derivatives, Polymers (Basel) 12 (2020) 1–13, https://doi.org/10.3390/polym12040972.
[19] A. Chiloeches, A. Funes, R. Cuervo-Rodríguez, et al., Biobased polymers derived from itaconic acid bearing clickable groups with potent antibacterial activity and negligible hemolytic activity, Polym. Chem. 12 (2021) 3190–3200, https://doi.org/10.1039/D1PY00098E.
[20] R. Tejero, B. Gutiérrez, D. López, et al., Copolymers of acrylonitrile with quaternizable thiazole and triazole side-chain methacrylates as potent antimicrobial and hemocompatible systems, Acta Biomater. 25 (2015), https://doi.org/10.1016/j.actbio.2015.07.037.
[21] R. Tejero, D. López, F. López-Fabal, et al., High efficiency antimicrobial thiazolium and triazolium side-chain polymethacrylates obtained by controlled alkylation of the corresponding azole derivatives, Biomacromolecules 16 (2015), https://doi.org/10.1021/acs.biomac.5b00427.
[22] R. Tejero, D. López, F. López-Fabal, et al., Antimicrobial polymethacrylates based on quaternized 1,3-thiazole and 1,2,3-triazole side-chain groups, Polym. Chem. 6 (2015) 3449–3459, https://doi.org/10.1039/C5PY00288E.
[23] M.W. Wang, H.H. Zhu, P.Y. Wang, et al., Synthesis of thiazolium-labeled 1,3,4-oxadiazole thioethers as prospective antimicrobials. In vitro and in vivo bioactivity and mechanism of action, J. Agric. Food Chem. 67 (2019) 12696–12708, https://doi.org/10.1021/acs.jafc.9b03952.
[24] S.A. Caldarelli, S. El Fangour, S. Wein, et al., New bis-thiazolium analogues as potential antimalarial agents: Design, synthesis, and biological evaluation, J. Med. Chem. 56 (2013) 496–509, https://doi.org/10.1021/jm3014585.
[25] Á. Sonseca, V. Hevilla-Talavera, D. López, et al., Glycerol-based enzymatically synthesized renewable polyesters: control of molecular weight, degree of branching and functional endgroups, Eur. Polym. J. 170 (2022), 111173, https://doi.org/10.1016/j.eurpolymj.2022.111173.
[26] M.L. Cerrada, R. Benavente, M. Fernández-García, et al., Crosslinking in metallocene ethylene-co-5,7-dimethylocta-1,6-diene copolymers initiated by electron-beam irradiation, Polymer (Guildf) 50 (2009), https://doi.org/10.1016/j.polymer.2009.01.006.
[27] H. Murata, R.R. Koepsel, K. Matyjaszewski, A.J. Russell, Permanent, non-leaching antibacterial surfaces—2: how high density cationic surfaces kill bacterial cells, Biomaterials 28 (2007) 4870–4879, https://doi.org/10.1016/j.biomaterials.2007.06.012.
[28] S. Kliewer, S.G. Wicha, A. Bröker, et al., Contact-active antibacterial polyethylene foils via atmospheric air plasma induced polymerisation of quaternary ammonium salts, Colloids Surf. B Biointerf. 186 (2020), 110679, https://doi.org/10.1016/j.colsurfb.2019.110679.
[29] J.C. Tiller, C.-J. Liao, K. Lewis, A.M. Klibanov, Designing surfaces that kill bacteria on contact, Proc. Natl. Acad. Sci. 98 (2001) 5981–5985, https://doi.org/10.1073/pnas.111143098.
[30] ASTM E2149-20, Standard Test Method for Determining the Antimicrobial Activity of Antimicrobial Agents Under Dynamic Contact Conditions, ASTM International, www.astm.org.
[31] Á.S. Olalla, V.H. Talavera, D.L. García, et al., Glycerol-based enzymatically synthesized renewable polyesters: control of molecular weight, degree of branching and functional endgroups, Eur. Polym. J. 170 (2022), 111173, https://doi.org/10.1016/j.eurpolymj.2022.111173.
[32] I.C. Becerril-Rodriguez, F. Claeyssens, Low methacrylated poly(glycerol sebacate) for soft tissue engineering, Polym. Chem. 13 (2022) 3513–3528, https://doi.org/10.1039/D2PY00212D.
[33] A. Vitale, S. Molina-Gutiérrez, W.S. Jennifer Li, et al., Biobased Composites by photoinduced polymerization of cardanol methacrylate with microfibrillated cellulose, Materials (Basel) 15 (2022), https://doi.org/10.3390/ma15010339.
[34] A. Muñoz-Bonilla, J. Zagora, D. Plachá, et al., Chemical hydrogels bearing thiazolium groups with a broad spectrum of antimicrobial behavior, Polymers (Basel) 12 (2020) 2853, https://doi.org/10.3390/polym12122853.
[35] C. Echeverría, A. Muñoz-Bonilla, R. Cuervo-Rodríguez, et al., Antibacterial PLA fibers containing thiazolium groups as wound dressing materials, ACS Appl. Bio Mater. 2 (2019) 4714–4719, https://doi.org/10.1021/acsabm.9b00923.
[36] V. Taresco, R.G. Creasey, J. Kennon, et al., Variation in structure and properties of poly(glycerol adipate) via control of chain branching during enzymatic synthesis, Polymer (Guildf) 89 (2016) 41–49, https://doi.org/10.1016/j.polymer.2016.02.036.
[37] S.I. Macías, G. Ruano, N. Borràs, et al., UV assisted photo reactive polyether-polyesteramide resin for future applications in 3D printing, J. Polym. Sci. 60 (2022) 688–700, https://doi.org/10.1002/pol.20210626.
[38] K. Lienkamp, K.-N. Kumar, A. Som, et al., "Doubly Selective" antimicrobial polymers: how do they differentiate between bacteria? Chem. – A Eur. J. 15 (2009) 11710–11714, https://doi.org/10.1002/chem.200802558.